The long-distance flight behavior of *Drosophila* supports an agent-based model for wind-assisted dispersal in insects

Katherine J. Leitch[a], Francesca V. Ponce[a], William B. Dickson[a], Floris van Breugel[a,1], and Michael H. Dickinson[a,2]

[a]Division of Biology and Bioengineering, California Institute of Technology, Pasadena, CA 91125

Edited by Alan Hastings, University of California, Davis, CA, and approved March 1, 2021 (received for review June 30, 2020)

Despite the ecological importance of long-distance dispersal in insects, its mechanistic basis is poorly understood in genetic model species, in which advanced molecular tools are readily available. One critical question is how insects interact with the wind to detect attractive odor plumes and increase their travel distance as they disperse. To gain insight into dispersal, we conducted release-and-recapture experiments in the Mojave Desert using the fruit fly, *Drosophila melanogaster*. We deployed chemically baited traps in a 1 km radius ring around the release site, equipped with cameras that captured the arrival times of flies as they landed. In each experiment, we released between 30,000 and 200,000 flies. By repeating the experiments under a variety of conditions, we were able to quantify the influence of wind on flies' dispersal behavior. Our results confirm that even tiny fruit flies could disperse ∼12 km in a single flight in still air and might travel many times that distance in a moderate wind. The dispersal behavior of the flies is well explained by an agent-based model in which animals maintain a fixed body orientation relative to celestial cues, actively regulate groundspeed along their body axis, and allow the wind to advect them sideways. The model accounts for the observation that flies actively fan out in all directions in still air but are increasingly advected downwind as winds intensify. Our results suggest that dispersing insects may strike a balance between the need to cover large distances while still maintaining the chance of intercepting odor plumes from upwind sources.

movement ecology | dispersal | *Drosophila* | navigation

If asked to picture a migrating insect, the first image that comes to mind might be a large charismatic species such as the monarch butterfly, whose seasonal movements across North America have inspired naturalists for centuries. However, as pointed out by David and Elizabeth Lack (1), our impression of insect migration is strongly biased toward large animals; many species are so small that their geographic relocations escape our attention, especially if their population densities are not strongly concentrated by geological features such as narrow mountain passes. As research using high-altitude traps (2) and upward-looking radar (3, 4) indicates, long-distance migration may be more ubiquitous and ecologically important among both large and small insects than previously appreciated (5, 6). Long-distance dispersal (i.e., the noncyclic movement from one area to another) is even harder to observe and study in small insects, because the events are not generally predictable, and the animals are far too small to be captured on radar or outfitted with tracking devices. The dispersal of small insects across a landscape has often been modeled as stochastic processes governed by diffusion and advection (7), processes that may underestimate the ability of the animals to actively maintain constant trajectories over large spatial scales. Understanding long-distance migration and dispersal is quite important, because these phenomena are responsible for biomass relocation on both local and global scales (8, 9). Furthermore, as insect population densities decline due to environmental degradation and climate change (10–12), understanding the dispersal capacity of insects and the behavioral algorithms that underlie them will be crucial in predicting the ecological impact of population decline.

Although not generally renowned for its capability to disperse over long distances, a series of release-and-recapture experiments over 40 y ago suggest that the fruit fly, *Drosophila melanogaster*, may be capable of movements on the order of 15 km in a single night, a distance equivalent to 6 million body lengths (13, 14). These experiments were conducted by releasing tens of thousands of fluorescently labeled flies in the evening and then censusing the contents of traps baited with yeast and banana placed at distant oases the next morning. Although these pioneering studies suggested that the dispersal capacity of *Drosophila* was much greater than previously estimated, they left open several critical questions. First, it was not clear whether individual flies dispersed in random directions or whether the population movement was biased by external conditions, such as the wind, geographical features, or celestial cues. Second, because the precise transit times of the flies were not known, it was impossible to estimate the actual groundspeeds used by the animals as they dispersed. To provide more clarity to these and other questions related to long-distance dispersal, we conducted a series of release-and-recapture experiments in the Mojave Desert. We equipped circular arrays of chemically baited traps with simple machine vision systems that captured the arrival times of flies as they landed and repeated the experiments under a variety of ambient wind conditions. The results provide key insight into the behavioral algorithms used by *Drosophila* while

Significance

Flying insects play a vital role in terrestrial ecosystems, and their decline over the past few decades has been implicated in a collapse of many species that depend upon them for food. By dispersing over large distances, insects transport biomass from one region to another, and thus, their flight behavior influences ecology on a global scale. Our experiments provide key insight into the dispersal behavior of insects and suggest that these animals employ a single algorithm that is functionally robust in both still air and under windy conditions. Our results will make it easier to study the ecologically important phenomenon of long-distance dispersal in a genetic model organism, facilitating the identification of cellular and genetic mechanisms.

Author contributions: K.J.L., F.v.B., and M.H.D. designed research; K.J.L., F.V.P., F.v.B., and M.H.D. performed research; W.B.D. contributed new reagents/analytic tools; K.J.L. and W.B.D. analyzed data; and K.J.L., W.B.D., and M.H.D. wrote the paper.

The authors declare no competing interest.

This article is a PNAS Direct Submission.

[1]Present address: The Department of Mechanical Engineering and Graduate Program for Neuroscience, University of Nevada, Reno, NV 89557.

[2]To whom correspondence may be addressed. Email: flyman@caltech.edu.

This article contains supporting information online at https://www.pnas.org/lookup/suppl/doi:10.1073/pnas.2013342118/-/DCSupplemental.

Published April 20, 2021.

dispersing in the wild and serve as the basis for a general agent-based model of wind-assisted dispersal in insects.

Results

To examine the long-distance flight behavior of *Drosophila*, we performed a series of release-and-recapture experiments on a dry lakebed, Coyote Lake, in the Mojave Desert (Fig. 1). We deployed a circular ring of traps, each equipped with a camera and baited with a fermenting solution of apple juice that actively produced CO_2 and ethanol, which attract flying flies (15). In most experiments ($n = 5$), we positioned 10 traps at a radius of 1 km; in one preliminary experiment, we placed the traps at a radius of 250 m. The mesh surface of the traps contained an array of inwardly pointed funnels that allowed entry, but limited egress, thus allowing us to count and identify the flies at the end of each experiment. (Fig. 1 *B* and *C*). An anemometer placed at the release site recorded instantaneous windspeed and direction. The number of flies released in each experiment ranged from ~30,000 to 200,000, consisting of both males and females.

We suspected that a small subset of flies would adopt trajectories leading directly to a trap (Fig. 1 *D*, *i*) but that the majority of those recaptured would first encounter a trap's odor plume and then track it upwind to find the source (Fig. 1 *D*, *ii*). Thus, we assume the trap count distributions to reflect two processes: 1) a dispersal flight over open space before a fly detects an odor plume and 2) a "cast-and-surge" upwind flight within the plume toward the trap (16). Wind is expected to impact both these processes by shaping the odor plumes and influencing the animals' groundspeed. Mean windspeed, which varied from release to release, influenced the final trap count distributions in a systematic manner (Fig. 2 *A* and *B*). Gentle winds resulted in a more uniform distribution of trap counts around the ring (Fig. 2*C*), whereas the distributions were skewed in a downwind direction in stronger winds. Despite this downwind bias in trapping distribution, some flies managed to arrive at crosswind and upwind traps in all but the strongest winds. Collectively, these results indicate that despite their small size, *Drosophila* are not simply advected by the wind as they disperse but rather have some capacity to fly in upwind and crosswind directions.

To determine if *Drosophila* actively regulate their groundspeed during dispersal, we compared arrival dynamics at downwind and upwind traps. This analysis was conducted on data collected from an experiment using a circular array of traps positioned 250 m from the release site, because the higher proportion (~2%) of flies recaptured at this shorter distance provided more arrival events. We pooled the camera data collected from the traps into two groups, representing the downwind and upwind sectors (Fig. 3, black versus cyan data). Although the pooled data from upwind and downwind traps differed with respect to the total number of flies captured, the time courses were remarkably similar. We also estimated the groundspeed of the first flies to arrive at each trap (hereafter, "first arrivers"), as these were individuals that most likely flew directly to the trap without an extended bout of upwind plume tracking. To score these first arrivers, we manually annotated the camera images to determine the first appearance of a *Drosophila*-shaped insect. These findings suggest that flies utilized a roughly similar groundspeed (0.94 ± 0.32 m · s^{-1}, mean ± SD, $n = 8$) despite having taken widely different trajectories relative to the prevailing wind of ~1.5 m · s^{-1}. This ability of flies to regulate groundspeed is well known from wind tunnel experiments (17–19) but had not been documented in the field.

By analyzing the data from experiments using traps set at 1 km, we could derive better estimates of flies' groundspeeds as well as examine the influence of the wind more accurately. As with the

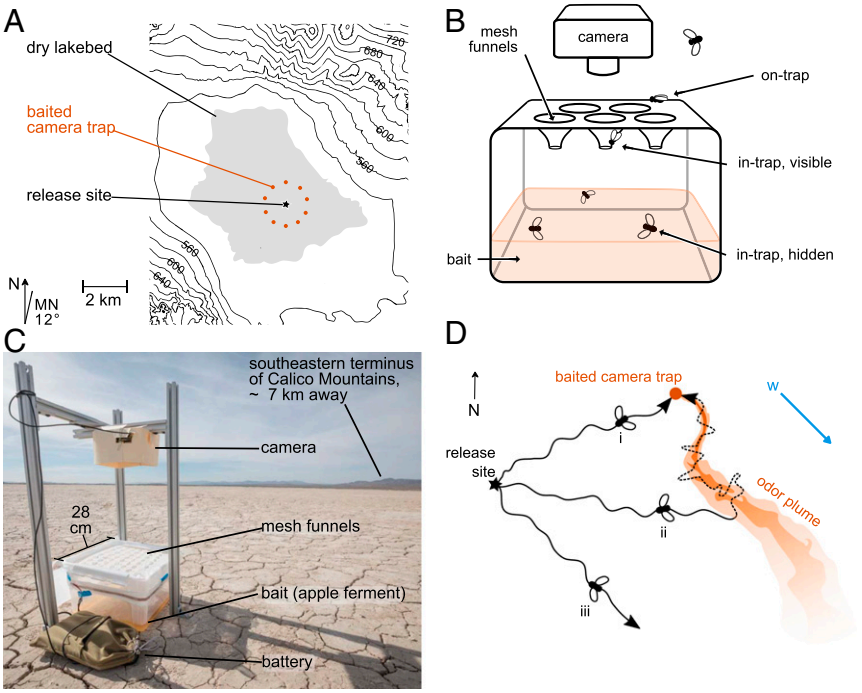

Fig. 1. Experimental design. (*A*) The experiments were conducted at Coyote Lake (gray), a dry lakebed in the Mojave Desert. Contours are in meters. We typically used 10 baited camera traps (orange) at a radius of 1 km from the release site (black star). North, N; magnetic north, MN. (*B*) Cartoon of trap, dimensions not to scale. The top mesh surface contained an array of funnels projecting inward toward the bait. Only five funnels are drawn; the actual traps had 60 funnels. The camera captures time-lapse images, monitoring the number of flies atop the trap (on-trap) and directly underneath the mesh top (in-trap, visible). The camera cannot detect flies deeper inside (in-trap, hidden). (*C*) Trap deployed on lakebed. (*D*) Key assumptions guiding experimental design. Wind (blue vector) advects a turbulent odor plume (orange) from each trap. Flies whose trajectory from the release site happens to intersect the plume near a trap (i) are likely to be among the earliest arrivers, owing to their relatively direct path. Flies that intercept a plume downwind of its source (ii) will follow a longer path before arriving at the trap (broken line). Many flies will not encounter a detectable plume (iii).

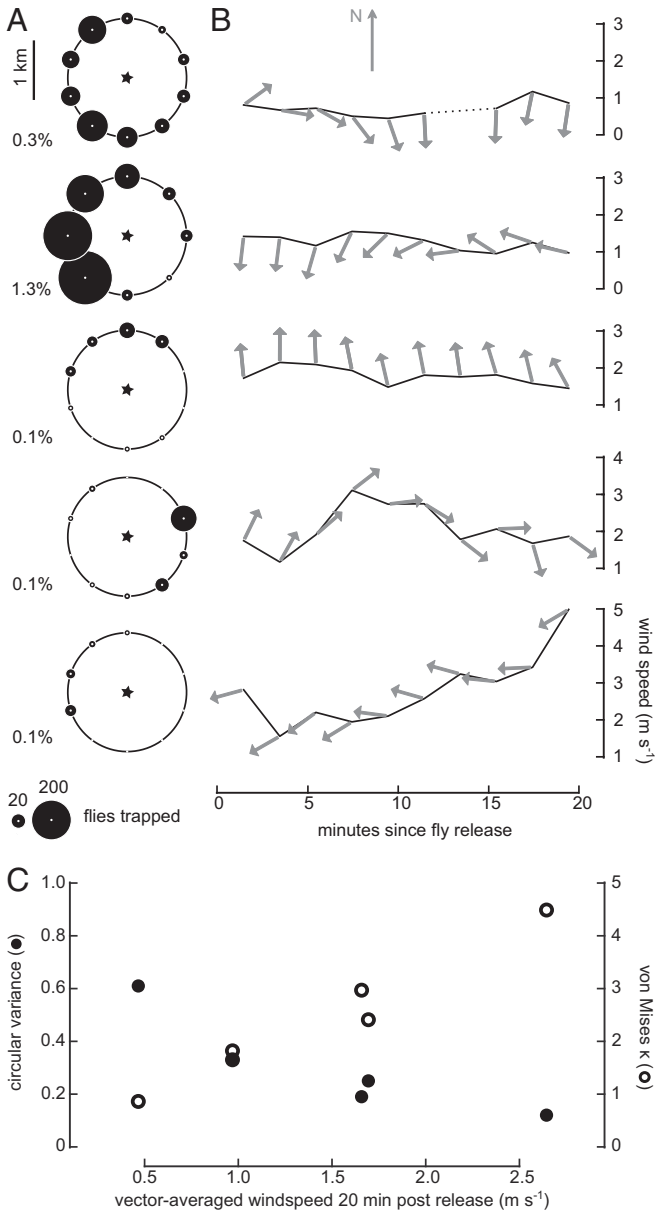

Fig. 2. Influence of wind on circular distribution of trapped flies. (*A*) Data from traps positioned 1 km away from the release site. Each row depicts the results of a different release. The area of each black circle indicates the number of flies caught in that trap by the end of each experiment. The five experiments are ordered according to the vector-averaged windspeed over the first 20 min following release. Recapture percentages, calculated using estimates of release populations, are indicated at the bottom left of each panel. (*B*) Windspeed and direction during the releases. Data were vector averaged in 2 min bins. Arrow lengths are fixed and point downwind; the position of each arrow's base along the ordinate indicates vector-averaged windspeed. We recorded wind data continuously, barring one brief anemometer failure shown in first row. (*C*) Circular variance (closed circles) and the von Mises parameter κ (open circles) are plotted as a function of vector-averaged windspeed for the five experiments.

250 m data, we manually annotated the camera images for the arrival of the first *Drosophila*-sized insect. Thirty different traps from the five experiments shown in Fig. 2 were amenable to this analysis. The camera data from nine of these 30 traps provided a sufficiently high signal-to-noise ratio that we could compare the manually annotated arrival times with an automated analysis, and the correspondence was reasonably good (*SI Appendix*, Fig. S1).

Using the arrival times, we estimated the average groundspeed along the trajectory from release site to trap, g_{traj}. From anemometer data, we determined the average headwind or tailwind that these first arrivers would have experienced during their flights, w_{traj} (Fig. 4*A*). Plotting g_{traj} against w_{traj} indicates the influence of the wind conditions (Fig. 4*B*). If the flies were simply advected by the wind, all the data should lie on a line running through the origin, with a slope of one. If the flies compensated groundspeed perfectly, then the data should fall about a horizontal line representing the average preferred groundspeed value. The distribution of field data suggests an intermediate behavior; flies exhibit some ability to actively regulate groundspeed at low windspeeds but tend to move with the wind as windspeed increases (Fig. 4*C*). Two data points showed unusually large values for groundspeed, and we suspect that these outliers were due to misidentification of some local fly-sized insects in our annotations. All subsequent analyses were performed on both the complete 30-point data set and after excluding these two outliers, but the exclusion did not alter any qualitative conclusions of our study. Fig. 4*C* also plots the comparable data collected from our release with traps set at 250 m. The overlapping distribution of data suggests that the flies executed the same preferred ground speed whether measured over 1 km or 250 m and that the interaction with the wind was governed by the same phenomena.

The cluster of groundspeed values measured when w_{traj} was near zero provides a rough estimate of the preferred groundspeed that flies use in the absence of any wind. This value, ~1 m · s^{-1}, is much higher than measurements of *Drosophila* flight velocities made in indoor wind tunnels (18, 20) but consistent with values made for flies flying in greenhouses (21). Obviously, any first arrivers that lingered at the release site, flew in a zig-zag manner, or had to work upwind long distances within the odor plume to reach the trap would have to have flown even faster to arrive at the recorded time (Fig. 4*A*). The high value for estimated groundspeed suggests that the flies—the first arrivers at least—must

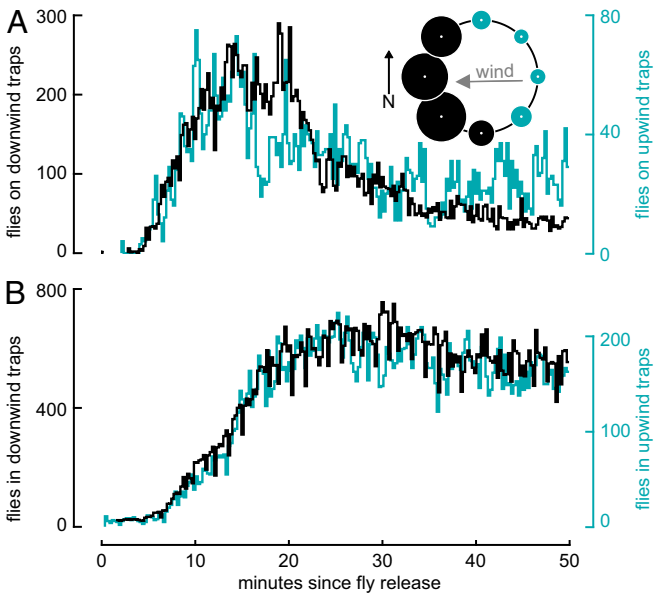

Fig. 3. In moderate winds, *Drosophila* regulate groundspeed. (*A*) During this experiment, traps were positioned at a 250 m radius from the release site. The vector-averaged windspeed was 1.5 m s^{-1}, almost due east (gray arrow). We define four traps as upwind (cyan circles) and four as downwind (black circles). The number of flies imaged on the trap surface (black), summed across all downwind traps for each time bin, is shown with the number of flies imaged on top of all upwind traps (cyan; note difference in scale). (*B*) From the same experiment, the number of flies visible within the upwind and downwind traps.

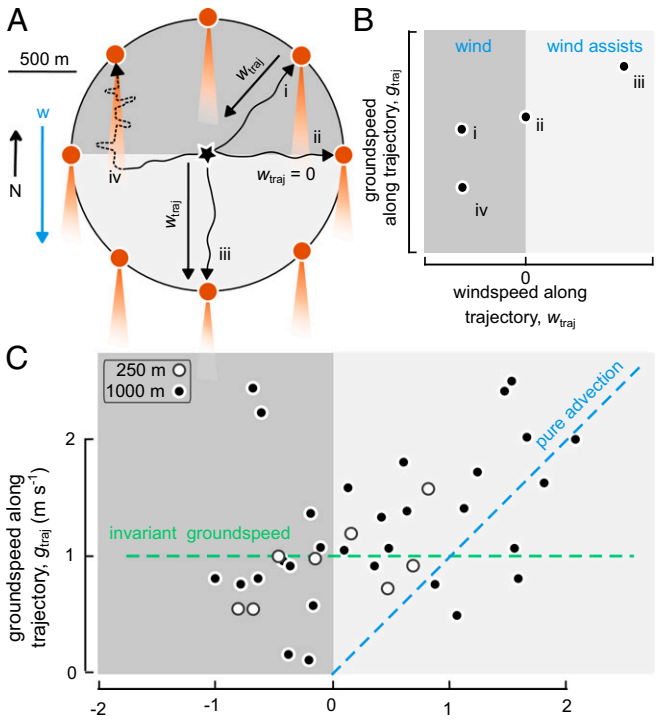

Fig. 4. Relationship between groundspeed and windspeed. (*A*) Hypothetical trajectories of four flies. Black vectors show the component of wind parallel to flight trajectories (w_{traj}). (*B*) For each fly in *A*, groundspeed along the trajectory (g_{traj}) is plotted as a function of w_{traj}. The value of g_{traj} will be underestimated for flight paths that do not intercept a plume near the trap (fly iv). Negative w_{traj} values (dark gray) denote trajectories opposed by the wind; positive (light gray) indicate trajectories assisted by wind. (*C*) Field measurements of g_{traj} and w_{traj}, from 30 1,000 m traps over the five experiments shown in Fig. 2 (black circles), superimposed with the relationships expected if flies were entirely advected by wind (blue) or maintained some preferred groundspeed (green). The white circles show comparable values of g_{traj} and w_{traj} derived from the 250 m trap experiment shown in Fig. 3.

have flown in rather straight trajectories between the release site and traps. If they had executed highly meandering paths, they could not have reached the traps at the recorded times using flight speeds that are biomechanically feasible.

Thus far, our results suggest that flies fan out in different directions when released, with at least some flies maintaining a roughly straight trajectory. Two basic mechanisms might explain how they maintain a straight path as they disperse. In the first, each fly chooses at random a constant heading (i.e., body orientation) relative to a celestial cue (22, 23). In the second, flies somehow actively maintain a constant trajectory (i.e., a straight path over the ground), perhaps by orienting to a distant visual landmark (24). These two hypotheses are distinct because a flying animal can move such that its longitudinal body axis (heading) is not aligned with its groundspeed vector (trajectory). Thus, an animal might maintain a constant heading while its trajectory varies or maintain a constant trajectory while its heading varies. The constant trajectory strategy has been observed in bumblebees during their nest-bound flights (25), and partial compensation has been observed in migratory noctuid moths (6). The constant heading hypothesis is consistent with radar observations of hoverflies' autumn migrations (26) and laboratory experiments showing that tethered flies will maintain a fixed, but arbitrary, orientation relative to patterns of polarized light (23, 27, 28) or the position of the sun (22).

To account for the influence of the wind, we propose a simple set of behavioral algorithms that collectively constitute an agent-based model that could explain the key features of our field data and is consistent with prior laboratory observations (Fig. 5, Model I). In our model, each fly maintains a constant heading and regulates groundspeed, but the groundspeed regulator, presumably mediated by vision (29), only operates on the velocity component oriented along the body axis. In other words, flies do not regulate sideslip but rather allow themselves to be advected sideways. Note, our analysis is based on measurements of the first arrivers—that we assume were lucky to choose a heading that carried them almost directly to a trap—and makes no attempt to model the complex phenomena associated with plume tracking. We developed a set of four agent-based models that all incorporated unregulated sideslip, but with different variations, thus creating a 2 × 2 matrix of two binary assumptions: 1) fixed random heading versus fixed random trajectory and 2) regulated longitudinal groundspeed versus unregulated groundspeed (Fig. 5). Fig. 6 *A*–*C* shows how three example flies, differing only in their chosen heading angle, would behave according to Model I (fixed heading with regulated groundspeed, Fig. 5) and how these would relate to the values of w_{traj} and g_{traj} available from field measurements (Fig. 4*B*). The illustrations in Fig. 6 *A*–*C* are equivalent to three simulations of Model I; running this simulation over the measured range of windspeeds and random directions generates a full set of predictions. The contours of the simulations are constrained by just three free parameters: the minimum (air_{min}) and maximum (air_{max}) airspeed achievable by the flies and the preferred groundspeed (g_{pref}) (Fig. 6*D*), values of which were chosen from measurements of *Drosophila* flying in a brightly lit greenhouse (21). Fig. 6*D* shows the output of Model I overlaid with the field data. The other three models implemented the alternate pairs of assumptions: Model II, unregulated groundspeed with fixed heading; Model III, regulated groundspeed with fixed trajectory; and Model IV, unregulated groundspeed with fixed trajectory.

To quantitatively compare their performance, we calculated the average pair-wise log likelihood ratio between Model I and each of the alternate models, determined using 40,000 bootstrap iterations (Fig. 6 *E*–*H*). The resultant distributions of log likelihood ratios indicate that Models I and III—both of which invoke groundspeed regulation—predict our field data equally well, in contrast to Models II and IV, which lack groundspeed regulation. To determine whether these conclusions were robust, we performed a sensitivity analysis across a wide range of values for each of the free parameters (*SI Appendix*, Figs. S2 and S3). For Models I and III, having three free parameters, we ran 864 simulations; for Models II and IV, with one free parameter, we ran 10 simulations. From this, we determined the parameter set for each model that best fit the field data. We then compared the individually optimized models, using the pair-wise log likelihood ratio described above (Fig. 6). As before, we found that the two models invoking groundspeed regulation better explained the field data than the models lacking this feature (*SI Appendix*, Fig. S4). The optimized parameter values were quite similar to the ones we had chosen a priori (Model I: $air_{max} = 2.0\ m \cdot s^{-1}$, $air_{min} = -0.5\ m \cdot s^{-1}$, $g_{pref} = 1.25\ m \cdot s^{-1}$; Model III: $air_{max} = 2.0\ m \cdot s^{-1}$, $air_{min} = -0.2\ m \cdot s^{-1}$, $g_{pref} = 1.5\ m \cdot s^{-1}$). Collectively, our results suggest that a relatively simple behavioral algorithm involving either fixed random heading or trajectory, regulated groundspeed, and unregulated sideslip can account for the salient features of dispersal behavior under a range of different wind conditions.

To compare our results with more traditional, analytic models of insect dispersal (7), we also simulated the expected distribution of g_{traj} and w_{traj} of flies arriving at a ring of traps if governed by the advection–diffusion equation. However, prior to determining a diffusion coefficient that best explains our results by brute force (Fig. 7), we can provide a rough estimate by noting that the rms displacement, R, of a particle moving by diffusion in the absence of advection is given by $R = \sqrt{4DT}$, where D is the

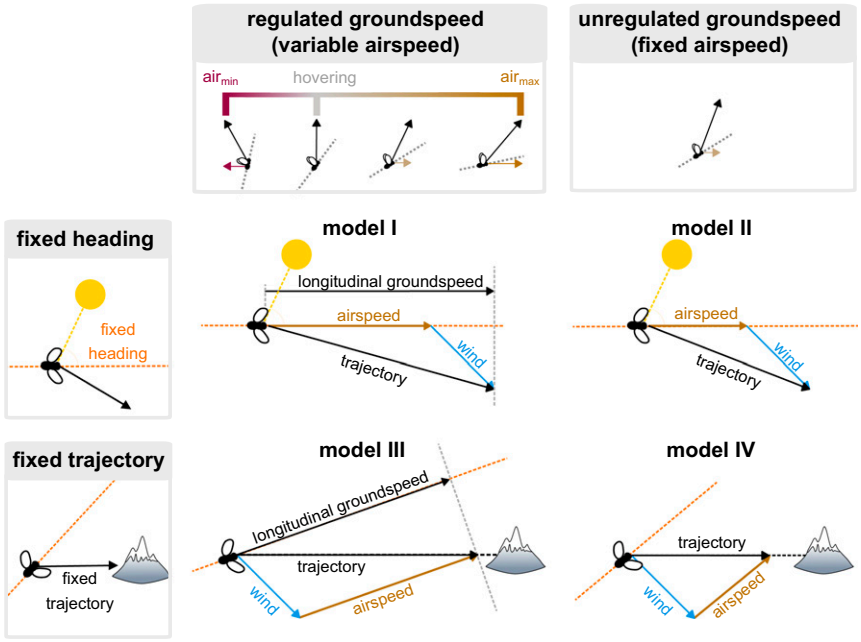

Fig. 5. Four behavioral models of wind-assisted dispersal. Cartoons depict how a fly's heading, trajectory, longitudinal groundspeed, and airspeed relate to the wind in each of four behavioral models. These models differ in azimuthal orientation strategies (rows) and in the presence or absence of groundspeed regulation (columns). In Model I, each fly maintains a fixed body angle relative to an external azimuthal reference (e.g., sun) and adjusts its airspeed, within limits, to achieve a preferred longitudinal groundspeed. The fly's longitudinal airspeed (brown) sums with the wind (blue), generating the fly's trajectory (black). Projecting the trajectory vector onto the fly's body axis gives the fly's longitudinal groundspeed, which the fly actively regulates. In Model II, each fly maintains a fixed heading as in the previous model but does not regulate longitudinal groundspeed. In Model III, each fly regulates longitudinal groundspeed and maintains a constant trajectory relative to some external azimuthal reference (e.g., mountain). In Model IV, each fly has unregulated groundspeed and a fixed trajectory.

diffusion constant and T is the time taken to reach R. We can rearrange this expression as $R/T = 4D/R$ and estimate R/T (which has units of velocity) as the flies' preferred groundspeed at zero windspeed (~1 m · s^{-1}, Fig. 4*C*). This calculation yields a diffusion coefficient of ~250 $m^2 \cdot s^{-1}$ for the 1 km trap data but a value of ~62 $m^2 \cdot s^{-1}$ for the 250 m trap data. This simple analysis suggests that data collected at 250 m and 1 km cannot be described by a single diffusion coefficient. To be governed by the same diffusivity, the flies arriving at the 250 m traps would have had to have flown approximately four times faster, or the flies arriving at the 1 km traps would have had to have flown ~0.25 times slower. What we instead observed is that flies used the same preferred groundspeed independent of the spatial scale of the experiment (Fig. 4*C*).

Our intuition based on this simple estimate of diffusivity was supported by a rigorous simulation of the advection–diffusion equation, in which the advection term was chosen from our field measurements (as in our agent-based simulations), and we determined the diffusion coefficient that optimized the fit between field data and model predictions. We first solved the advection–diffusion equation on a circular grid with an absorbing outer boundary but then transformed the data into probability functions of w_{traj} and g_{traj}, as in our agent-based models, which we could then directly compare to our field data (*SI Appendix*). The solutions that yielded the lowest log Bayes factors are shown in Fig. 7, for both the 250 m and 1 km trap data. The diffusion coefficients determined in this fashion (70 $m^2 \cdot s^{-1}$ for the 250 m data and 300 $m^2 \cdot s^{-1}$ for 1 km data) were remarkably similar to the values predicted by our simple algebraic estimate described above and underscore the fact that a single diffusion coefficient does not well explain the data collected at the two different spatial scales, simply because the first arrivers were traveling at the same speed in the two cases. Our field data are thus not well approximated by a simple diffusion–advection model and are more consistent with the assumptions of our agent-based models.

In addition to evaluating our models with respect to trap–arrival dynamics, we also tested their ability to predict the overall angular distribution of trap counts with respect to the wind (Fig. 2*C*). Our simulations provide angles of each fly's trajectory, so we examined the circular variance of these as a function of windspeed for each of the four agent-based models plus that of the advection–diffusion model. All five models show a narrowing of the population trajectories as wind increases (*SI Appendix*, Fig. S5), qualitatively consistent with our field data. However, we made no attempt to model the process of plume tracking, which we expect to strongly affect final trap counts in the field.

Although the simulated flies in our agent-based models choose an initial heading at random, they do not incorporate any subsequent stochastic changes in heading as is often used to model insect dispersal (30). To explore the influence of stochastic heading changes, we performed an additional set of simulations in which flies followed the rules of ground speed regulation and unregulated sideslip, but they also changed heading randomly according to prescribed statistics. To encompass a broad range of stochastic behavior, we varied the statistics of heading changes in two independent ways: (1) we modeled the distributions of run lengths with power law statistics (31) with μ values of 1, 1.5, and 2 and run length intervals ranging from 1 s to 1,000 s and (2) chose each new heading from a von Mises distribution with κ values (inverse of circular variance) of 500, 10, 1, and 0.1. Thus, these simulations constituted a 3-by-4 matrix of stochastic variations on Model I (*SI Appendix*, Fig. S6). Note that the bottom row of simulations for which $\kappa = 500$ converge, as expected, on our original agent-based Model I (Fig. 6*E*), because the circular variance is so low that the flies choose the same initial heading each time they change direction, thereby continuing in a straight line. The effect of changing the

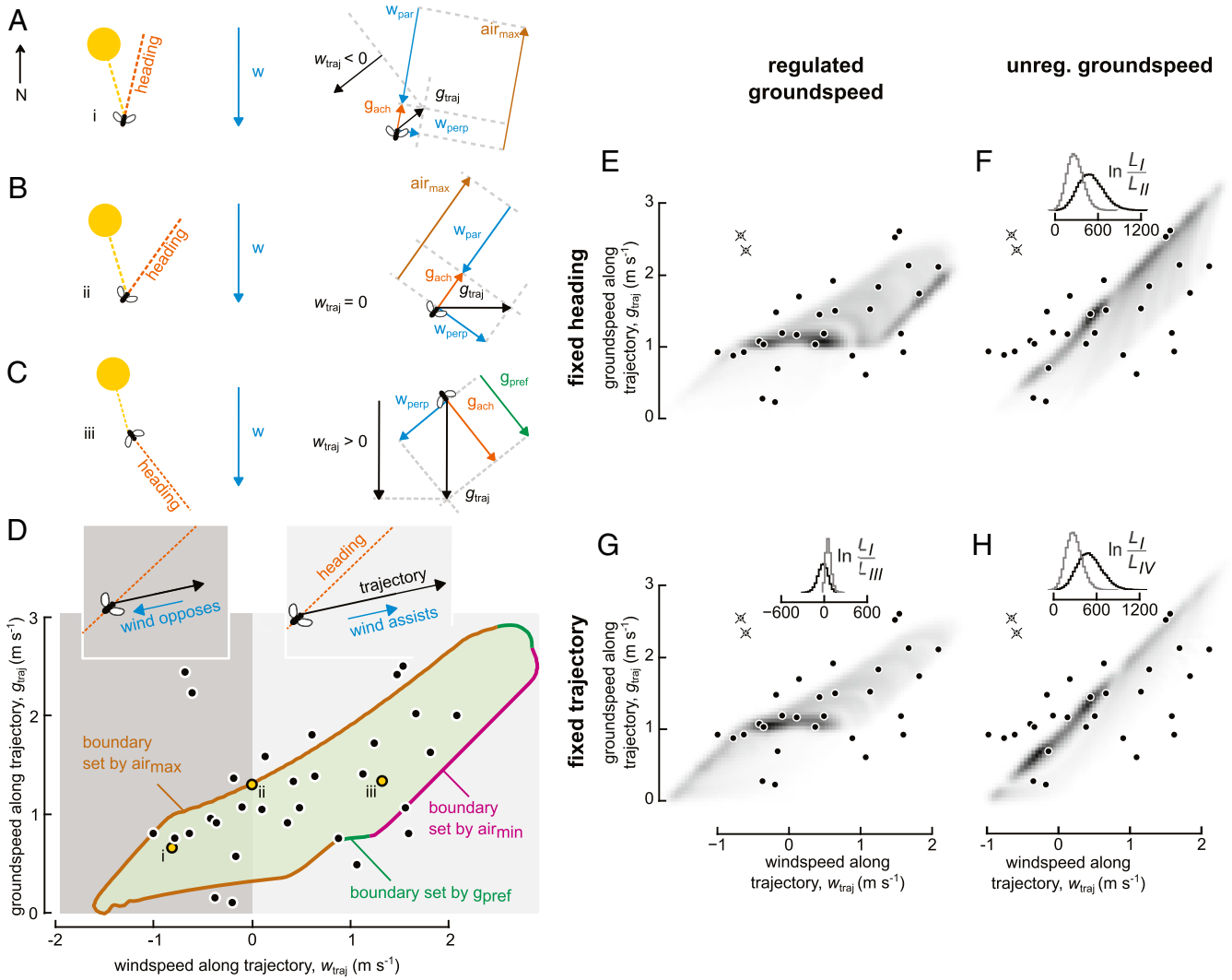

Fig. 6. Field data support dispersal models integrating groundspeed regulation with either fixed heading or trajectory. (*A–C*) How Model I might generate trajectories i through iii depicted in Fig. 4*A*. (*A*) Because fly i holds its heading nearly due north, a large component of the wind (w_{par}) constitutes a headwind. By exerting maximum airspeed against w_{par}, the fly achieves a modest longitudinal groundspeed (g_{ach}). The vector sum of g_{ach} and w_{perp} yields the fly's groundspeed (g_{traj}), the magnitude of which is one of the field-measurable parameters. (*B*) Fly ii orients its body ~35° from north; applying the maximum airspeed along this heading results in a trajectory due east. The net trajectory is entirely perpendicular to the wind, yielding $w_{traj} = 0$. (*C*) Fly iii orients its body ~40° from south; in this case, w_{par} is infinitesimally small, and the fly can achieve its preferred groundspeed (g_{pref}). Summed with w_{perp}, this yields a g_{traj} vector pointing due south and a w_{traj} vector of the same magnitude as the wind. (*D*) The relationship between w_{traj} and g_{traj}, simulated over a range of windspeeds and wind directions, with $g_{pref} = 1.0$ m · s^{-1}, $air_{min} = -0.2$ m · s^{-1}, and $air_{max} = 1.8$ m · s^{-1}. The three yellow points indicate the approximate values from the example simulated flies i, ii, and iii schematized in *A*, *B*, and *C* above, assuming a windspeed of 1.3 m · s^{-1}. The 99% contour from all simulations is filled in green. Boundaries of this contour are constrained by model parameters air_{max} (brown), air_{min} (purple), and g_{pref} (teal). Black points indicate field measurements. (*E–H*) The four behavioral models, simulated over a wide range of wind conditions, generate distinct relationships between the two field-measurable parameters. Grayscale shading shows each models' normalized probability density function (PDF). Field measurements are plotted over each model's PDF; likelihood values at each point were compared pairwise between models. In an alternate analysis, two possible outliers (overlaid with crosses) were excluded. (*E*) PDF generated by Model I. (*F*) PDF generated by Model II. (*Inset*) Bootstrapping the field data over 40,000 iterations generated a distribution of log likelihood ratios comparing Models I and II. Positive values denote iterations in which Model I predicted the resampled data better than did Model II. The mean of this distribution was 499 (black) or, excluding outliers, 282 (gray). (*G*) PDF of model III. (*Inset*) Comparison of Models I and III. Distribution mean is −20 and, excluding outliers, 61. (*H*) PDF from Model IV. (*Inset*) comparison of Models I and IV. Distribution mean is 504 and, excluding outliers, 288.

power law slope, μ, is intuitive in that a bias toward short run times (μ = 2) augments the influence of advection, whereas bias toward very long run times (μ = 1) allows many simulated flies to make headway in the upwind direction (i.e., higher probability density for $w_{traj} < 0$), again converging on the assumptions of our original model. To compare the performance of the models with added stochasticity to our original, we again calculated the average pair-wise log likelihood ratio between Model I (Fig. 6*E*) and each of the alternative models (*SI Appendix*, Fig. S6, *Insets*). The results indicate that the introduction of stochastic turns can slightly improve the correspondence between our model and the field data provided that run lengths are very long (i.e., μ = 1). The slight improvement in model fit with μ = 1 is likely due to a downward shift in the probability of g_{traj} values that is most apparent at low κ values. This makes sense intuitively, because even infrequent changes in direction will lower the net groundspeed of some flies measured when they reach the simulated trap location. This effect might explain why we detected approximately five first arrivers in

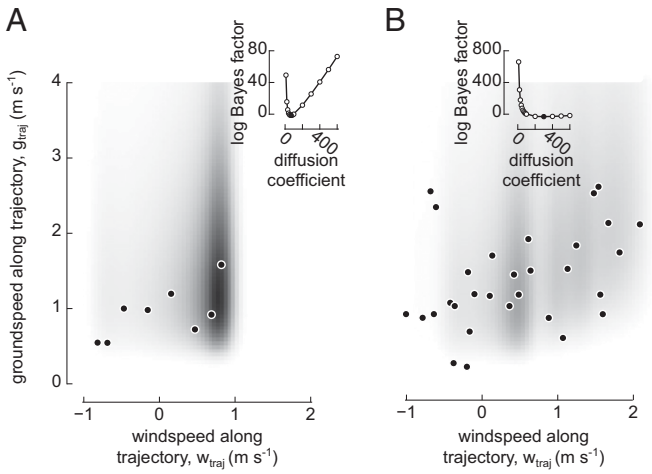

Fig. 7. Predictions of release-and-recapture data using advection–diffusion model. Each panel plots normalized probability density functions for values of w_{traj} and g_{traj} predicted from simulations of the advection–diffusion equation over a circular domain representing the release site and circular trap array (*SI Appendix*). (*A*) Simulation results (gray density) compared to field data (points) for the release experiment performed with traps at 250 m (Fig. 3). The results shown are based on the measured wind conditions after applying a Gaussian kernel. The value of the diffusion coefficient that resulted in the best fit with the field data was 70 $m^2 \cdot s^{-1}$. The inset shows the metric for the fit (log Bayes factor) as a function of different diffusion coefficients. The model is particularly bad at predicting the data generated by flies flying upwind ($w_{traj} < 0$) at their preferred groundspeed ($w_{traj} \sim 1$). (*B*) As in *A* but for the complete set of trap data collected at 1 km. As in our agent-based simulations (Fig. 6 *E–H*), these simulations used a composite of windspeeds measured during all five experiments. In the 1 km case, the data were best fit by a diffusion coefficient of 300 $m^2 \cdot s^{-1}$.

our field data that flew at a much lower-than-expected groundspeed than predicted by our original model. Thus, within limits, the introduction of stochastic changes in direction can improve the predictions of our agent-based model, but the results nevertheless support the hypothesis that *Drosophila* are capable of maintaining relatively straight headings over kilometer-scale distances.

Discussion

Our results provide evidence that an agent-based model in which flies maintain a constant heading and preferred longitudinal ground speed while not regulating sideslip can explain salient features of dispersal in an open landscape. Agent-based models in which each animal follows a finite set of rules are not necessarily incompatible with statistical models such as the advection–diffusion equation, in which animals move according to a random Brownian process. However, in this particular case, the behavior of the first arriver flies at our field traps was not consistent with Brownian motion because flies appear to maintain a preferred groundspeed that is scale independent. While not negating the utility of advection–diffusion models in describing insect motion under many conditions—in a more spatially complicated, sensory landscape, for example—our results suggest that when released in an open area, *Drosophila* execute a set of behavioral algorithms that appear largely optimized for long-distance dispersal rather than local search. Further, our experiments confirm the earlier results of Coyne and coworkers (13), suggesting that *Drosophila* can disperse over many kilometers in a single flight.

Our results indicate that dispersing *Drosophila* actively regulate their longitudinal groundspeed to a value of ~1 $m \cdot s^{-1}$ (3.6 $km \cdot hr^{-1}$). Fully fed, tethered flies can fly for up to 3 h (24), a value that is consistent with measurements of metabolic rate and aerodynamic power requirements (32). This suggests that a single fly could cover ~12 km without the need for refueling, a distance of about 4.8 million body lengths. Even if this value represents an extreme performance estimate, it nevertheless demonstrates a surprising dispersal capacity for a small, 1 mg insect. At the higher groundspeeds we measured under windy conditions (~2.5 $m \cdot sec^{-1}$), the dispersal distance estimate for a single flight increases to ~30 km. Flies could almost certainly disperse much further in an uncontrolled fashion in more extreme conditions, especially if they were carried well above the boundary layer into higher elevations where they catch prevailing winds (33). Presumably, it is just such uncontrolled events that resulted in the colonization of isolated oceanic islands (34).

Many animals localize food by moving upwind within advected odor plumes (16), a behavior termed odor-mediated anemotaxis. This behavior typically involves an iterative sequence of upwind surges when odor is detected, interspersed with crosswind casts when the odor is lost. Although we could not directly observe plume tracking in our field experiments, *Drosophila* readily exhibit such behavior in wind tunnels (35, 36). Whereas the utility of the cast-and-surge algorithm is obvious once an animal encounters a plume, the best strategy before it detects an odor is less clear and may depend on wind conditions (37, 38) and—just as importantly—on the natural history of each particular species. Some insects, such as the cabbage root fly, fly upwind when experiencing an odorless background flow (39). This might seem logical, simply because if an animal detects an odor, its source must be upwind. On the other hand, by flying upwind, an animal limits itself to odor targets that reside in a narrow sector directly ahead. Tsetse flies fly downwind prior to detecting an odor plume (40), possibly because this allows them to cover a greater distance while searching for hosts. Another strategy, observed in both desert ants (41) and albatross (42), is to deliberately move crosswind so as to intercept the largest number of upwind plumes. Another strategy, found in *Agrotis* moths, is to search upstream if they detect a female pheromone but search crosswind or downwind if they do not (43). These same experiments suggest that search patterns may shift to a more random strategy if a target odor is not detected within some specified time. In our experiments, we observed that *Drosophila* fan out in all directions at low windspeeds, similar to the behavior reported in gypsy moths (44), while at higher speeds, the flies were biased downwind. The behavior we observed, and the model we propose, may be viewed as a compromise between the need to find an attractive odor plume and the goal of using the wind to increase dispersal distance. By not regulating sideslip, the flies allow themselves to be directed downwind, but by regulating longitudinal groundspeed, they maintain some crosswind component that might increase the probability of encountering an upwind plume.

Although we captured flies at odor-baited traps, there is some possibility that the flies arrived without having tracked its associated plume upwind. If 100,000 flies fanned out evenly in all directions from the release site, they would reach the perimeter of the trap radius at a linear density of ~16 flies per meter. If we liberally assume that a fly might be able to see a trap from a distance of 10 m, then it is possible that ~320 flies would pass near enough to a trap that they might land on it without needing to follow the odor plume. Thus, we may have only trapped flies that happened to choose trajectories that carried them near one of the traps. There are several arguments against this interpretation. First, our coarse estimates for how many flies came within the visual detection range of the traps are almost certainly an overestimate as it assumes that all the flies flew within 1 to 2 m of the ground where they could encounter the trap. *Drosophila spp.* have been observed at high density in 200 m–high aerial traps (2), and it is possible that many of the flies in our experiments rose well above the ground after release. Second, laboratory experiments indicate that flying flies are not attracted to land on visual objects until after they have encountered an attractive odor (36); it thus seems reasonable to assume that the flies would have made some contact with the plume before landing on the trap.

Of the agent-based models we tested, the two that combined longitudinal groundspeed regulation with either fixed heading or fixed trajectory (Models I and III) performed best in predicting our field data. Of these two, we believe that the fixed heading model is the most biologically plausible as this is consistent with laboratory experiments showing that flies adopt arbitrary headings relative to patterns of skylight polarization and sun position. Tethered *Drosophila* do steer toward large conspicuous visual objects (30)—a reflex called stripe fixation. However, although the lakebed is surrounded by some ridges (Fig. 1*A*), none contain vertical features that seem prominent enough to elicit a strong fixation response from the release site. Further, a fixation response to one or two geological features could not easily explain how flies fan out in many directions. As argued elsewhere, stripe fixation is better interpreted as a transient attraction toward nearby objects rather than a long-distance orientation behavior (45).

Dispersing *Drosophila* use celestial cues not as a compass to go in a preferred direction but rather simply as a means of holding an arbitrary orientation (i.e., menotaxis). In this regard, flies' use of the sky compass system is similar to dung beetles, which maintain a straight trajectory away from the dung pile (46), but not like monarch butterflies, which use the sun compass to fly in a particular direction (47). However, as has been pointed out by Honkanen et al. (48), the alteration in central complex circuitry that would be required to transform compass-based random dispersal behavior into seasonal migration might be quite subtle, and the two behaviors are perhaps better viewed as points on a continuum.

We deliberately chose to conduct our experiments on a flat, featureless, dry lakebed to simplify the external factors that might influence dispersal behavior; however, we acknowledge that our experiments were artificial in a number of ways. First, *D. melanogaster* is a cosmopolitan species that originated in Africa (49). Thus, we can infer little regarding the species-specific behavior of the flies as it relates to their ancestral habitat. Instead, our observations more likely shed light on deeply rooted behavioral algorithms that are shared by many insects and not the result of recent evolutionary processes (45). Second, our experiments forced a rapid, mass exodus, whereas dispersal within the normal life history of flies is more likely a choice influenced by a complex interaction of internal and external factors. Even in species in which dispersal is not associated with distinct morphological changes (50), it may be anticipated by physiological modifications (51). Further, laboratory populations subjected to strong selection for dispersal ability (as measured in walking assays) exhibit heritable changes in behavior (52); thus, it is possible that distinct populations of flies might respond differently in a mass release depending upon their genetic composition. However, upon emergence, we did maintain the flies ad libitum on a protein-deprived diet. This was a deliberate attempt to proffer them an ample energy source while also providing a strong motivation to search elsewhere for protein-rich food (53). The fact that the vast majority of flies left the containers upon release gives us some confidence that the animals were not inhibited from initiating long-distance flight by either physiological or genetic factors and that our feeding regime may have had the desired effect.

In summary, we propose a model of wind-assisted dispersal in which each insect chooses and maintains a random heading and regulates its longitudinal groundspeed but tolerates wind-induced sideslip. While undoubtedly simplistic, the advantage of our model is that it can explain dispersal behavior under a variety of wind conditions without requiring that any individual animal change its behavioral set point as a function of windspeed. It thus represents a biologically feasible "rule-of-thumb" that yields a desired behavioral outcome without requiring sophisticated neural computations. Although derived from measurements on *Drosophila*, we suggest that the model might explain the dispersal behavior of many flying insects with roughly similar natural histories.

Materials and Methods

Fly Release and Recapture. We performed a series of release-and-recapture experiments using a population of laboratory-reared *D. melanogaster* on a dry lakebed (Coyote Lake) in the Mojave Desert. We deployed a circular ring of traps, each equipped with a downward-facing camera (Raspberry Pi) and baited with fermenting apple juice. In five experiments, we positioned 10 traps at a radius of 1 km; in one preliminary experiment, we placed the traps at a radius of 250 m. The mesh surface of the traps contained an array of inwardly pointed funnels, allowing us to count and identify the flies at the end of each experiment. (Fig. 1 *B* and *C*). An anemometer (Met One, direction sensor 020C, speed sensor 010C) placed at the release site recorded the time course of windspeed and direction in each experiment. The number of flies released in each experiment ranged from ~30,000 to 200,000. In addition to counting the flies that had arrived at each trap, we also scored the arrival times of the first flies to land on each trap via manual inspection of time-stamped camera images and in some cases using custom-written machine vision software (54). For details, see the article text and *SI Appendix*.

Agent-Based Models. To help interpret our results, we developed agent-based models in which each fly maintains a random constant azimuthal orientation but is advected sideways by the wind. We developed four different models that all incorporated unregulated sideslip but differed with respect to whether the flies maintained a constant heading or constant trajectory and whether they regulated longitudinal groundspeed or not. We simulated the output of the models using ~45,000 permutations in which each fly chose a different heading or trajectory and was subjected to a wind magnitude derived from a distribution based on our field measurements (54). For details, see the article text and *SI Appendix*.

Advection–Diffusion Model. We also simulated the expected distribution of g_{traj} and w_{traj} for flies arriving at a ring of traps if governed by the advection–diffusion equation. Using measured values for wind, we determined the diffusion coefficient that optimized the fit between field data and model predictions. We first solved the advection–diffusion equation on a circular grid with an absorbing outer boundary but then transformed the data into probability functions of w_{traj} and g_{traj}, as in our agent-based models. The advection–diffusion equation was solved using the FEniCS platform (https://fenicsproject.org) (54). For details, see *SI Appendix*.

Data Availability. All data and analysis code used in this paper are available for download at https://github.com/kateleitch/drosophila_wind_assisted_dispersal.

ACKNOWLEDGMENTS. We thank Massimo Vergassola (University of California San Diego), who was principal investigator on a grant from the Simons Foundation (71582123) that funded the initial stages of this project. This work was also supported by the NSF (IOS 1547918). Román Corfas, Ainul Huda, Alysha de Souza, Johan Melis, and Aubrey Goldsmith participated in data collection. Annie Rak contributed to preliminary modeling efforts. Bob Verish provided guidance for safely accessing Coyote Lake, and the Barstow Field Office of the Bureau of Land Management permitted our use of this field site.

1. D. Lack, E. Lack, Migration of insects and birds through a Pyrenean pass. *J. Anim. Ecol.* **20**, 63–67 (1951).
2. J. W. Chapman, D. R. Reynolds, A. D. Smith, E. T. Smith, I. P. Woiwod, An aerial netting study of insects migrating at high altitude over England. *Bull. Entomol. Res.* **94**, 123–136 (2004).
3. J. W. Chapman, D. R. Reynolds, A. D. Smith, Vertical-looking radar: A new tool for monitoring high-altitude insect migration. *Bioscience* **53**, 503–511 (2003).
4. J. W. Chapman, V. A. Drake, D. R. Reynolds, Recent insights from radar studies of insect flight. *Annu. Rev. Entomol.* **56**, 337–356 (2011).
5. J. W. Chapman *et al.*, Flight orientation behaviors promote optimal migration trajectories in high-flying insects. *Science* **327**, 682–685 (2010).
6. J. W. Chapman *et al.*, Wind selection and drift compensation optimize migratory pathways in a high-flying moth. *Curr. Biol.* **18**, 514–518 (2008).
7. P. M. Kareiva, Local movement in herbivorous insects: Applying a passive diffusion model to mark-recapture field experiments. *Oecologia* **57**, 322–327 (1983).
8. G. Hu *et al.*, Mass seasonal bioflows of high-flying insect migrants. *Science* **354**, 1584–1587 (2016).
9. S. Bauer, B. J. Hoye, Migratory animals couple biodiversity and ecosystem functioning worldwide. *Science* **344**, 1242552 (2014).
10. C. A. Hallmann *et al.*, More than 75 percent decline over 27 years in total flying insect biomass in protected areas. *PLoS One* **12**, e0185809 (2017).

11. D. Goulson, The insect apocalypse, and why it matters. *Curr. Biol.* **29**, R967–R971 (2019).
12. R. van Klink *et al*., Meta-analysis reveals declines in terrestrial but increases in freshwater insect abundances. *Science* **368**, 417–420 (2020).
13. J. A. Coyne *et al*., Long-distance migration of Drosophila. *Am. Nat.* **119**, 589–595 (1982).
14. J. S. Jones, S. H. Bryant, R. C. Lewontin, J. A. Moore, T. Prout, Gene flow and the geographical distribution of a molecular polymorphism in Drosophila pseudoobscura. *Genetics* **98**, 157–178 (1981).
15. F. van Breugel, A. Huda, M. H. Dickinson, Distinct activity-gated pathways mediate attraction and aversion to CO_2 in Drosophila. *Nature* **564**, 420–424 (2018).
16. K. L. Baker *et al*., Algorithms for olfactory search across species. *J. Neurosci.* **38**, 9383–9389 (2018).
17. C. T. David, The relationship between body angle and flight speed in free-flying Drosophila. *Physiol. Entomol.* **3**, 191–195 (1978).
18. V. Medici, S. N. Fry, Embodied linearity of speed control in Drosophila melanogaster. *J. R. Soc. Interface* **9**, 3260–3267 (2012).
19. S. B. Fuller, A. D. Straw, M. Y. Peek, R. M. Murray, M. H. Dickinson, Flying Drosophila stabilize their vision-based velocity controller by sensing wind with their antennae. *Proc. Natl. Acad. Sci. U.S.A.* **111**, E1182–E1191 (2014).
20. A. D. Straw, S. Lee, M. H. Dickinson, Visual control of altitude in flying Drosophila. *Curr. Biol.* **20**, 1550–1556 (2010).
21. S. A. Combes, D. E. Rundle, J. M. Iwasaki, J. D. Crall, Linking biomechanics and ecology through predator-prey interactions: Flight performance of dragonflies and their prey. *J. Exp. Biol.* **215**, 903–913 (2012).
22. Y. M. Giraldo *et al*., Sun navigation requires compass neurons in Drosophila. *Curr. Biol.* **28**, 2845–2852.e4 (2018).
23. T. L. Warren, P. T. Weir, M. H. Dickinson, Flying *Drosophilamelanogaster* maintain arbitrary but stable headings relative to the angle of polarized light. *J. Exp. Biol.* **221**, jeb177550 (2018).
24. K. G. Götz, Course-control, metabolism and wing interference during ultralong tethered flight in Drosophila melanogaster. *J. Exp. Biol.* **128**, 35–46 (1987).
25. J. R. Riley *et al*., Compensation for wind drift by bumble-bees. *Nature* **400**, 126 (1999).
26. B. Gao *et al*., Adaptive strategies of high-flying migratory hoverflies in response to wind currents. *Proc. Biol. Sci.* **287**, 20200406 (2020).
27. P. T. Weir, M. H. Dickinson, Flying Drosophila orient to sky polarization. *Curr. Biol.* **22**, 21–27 (2012).
28. R. Wolf, B. Gebhardt, R. Gademann, M. Heisenberg, Polarization sensitivity of course control in Drosophila melanogaster. *J. Comp. Physiol.* **139**, 177–191 (1980).
29. C. T. David, Compensation for height in the control of groundspeed by Drosophila in a new, 'barber's pole' wind tunnel. *J. Comp. Physiol.* **147**, 485–493 (1982).
30. P. M. Kareiva, N. Shigesada, Analyzing insect movement as a correlated random walk. *Oecologia* **56**, 234–238 (1983).
31. A. M. Reynolds, C. J. Rhodes, The Lévy flight paradigm: Random search patterns and mechanisms. *Ecology* **90**, 877–887 (2009).
32. F. O. Lehmann, M. H. Dickinson, The changes in power requirements and muscle efficiency during elevated force production in the fruit fly Drosophila melanogaster. *J. Exp. Biol.* **200**, 1133–1143 (1997).
33. D. R. Reynolds, J. W. Chapman, V. A. Drake, "Riders on the wind: The aeroecology of insect migrants" in *Aeroecology*, P. B. Chilson, W. F. Frick, J. F. Kelly, F. Liechti, Eds. (Springer International Publishing, Cham, 2017), pp. 145–178.
34. H. L. Carson, K. Y. Kaneshiro, Drosophila of Hawaii: Systematics and ecological genetics. *Annu. Rev. Ecol. Syst.* **7**, 311–345 (1976).
35. S. A. Budick, M. H. Dickinson, Free-flight responses of Drosophila melanogaster to attractive odors. *J. Exp. Biol.* **209**, 3001–3017 (2006).
36. F. van Breugel, M. H. Dickinson, Plume-tracking behavior of flying Drosophila emerges from a set of distinct sensory-motor reflexes. *Curr. Biol.* **24**, 274–286 (2014).
37. D. B. Dusenbery, Optimal search direction for an animal flying or swimming in a wind or current. *J. Chem. Ecol.* **15**, 2511–2519 (1989).
38. M. W. Sabelis, P. Schippers, Variable wind directions and anemotactic strategies of searching for an odour plume. *Oecologia* **63**, 225–228 (1984).
39. S. Finch, G. Skinner, Upwind flight by the cabbage root fly, Delia radicum. *Physiol. Entomol.* **7**, 387–399 (1982).
40. G. Gibson, M. J. Packer, P. Steullet, J. Brady, Orientation of tsetse flies to wind, within and outside host odour plumes in the field. *Physiol. Entomol.* **16**, 47–56 (1991).
41. C. Buehlmann, P. Graham, B. S. Hansson, M. Knaden, Desert ants locate food by combining high sensitivity to food odors with extensive crosswind runs. *Curr. Biol.* **24**, 960–964 (2014).
42. G. A. Nevitt, M. Losekoot, H. Weimerskirch, Evidence for olfactory search in wandering albatross, Diomedea exulans. *Proc. Natl. Acad. Sci. U.S.A.* **105**, 4576–4581 (2008).
43. A. M. Reynolds, D. R. Reynolds, A. D. Smith, G. P. Svensson, C. Löfstedt, Appetitive flight patterns of male Agrotis segetum moths over landscape scales. *J. Theor. Biol.* **245**, 141–149 (2007).
44. J. S. Elkinton, R. T. Cardé, Appetitive flight behavior of male gypsy moths (Lepidoptera: Lymantridae). *Environ. Entomol.* **12**, 1702–1707 (1983).
45. M. H. Dickinson, Death Valley, Drosophila, and the Devonian toolkit. *Annu. Rev. Entomol.* **59**, 51–72 (2014).
46. M. Dacke, B. El Jundi, The dung beetle compass. *Curr. Biol.* **28**, R993–R997 (2018).
47. H. Mouritsen, B. J. Frost, Virtual migration in tethered flying monarch butterflies reveals their orientation mechanisms. *Proc. Natl. Acad. Sci. U.S.A.* **99**, 10162–10166 (2002).
48. A. Honkanen, A. Adden, J. da Silva Freitas, S. Heinze, The insect central complex and the neural basis of navigational strategies. *J. Exp. Biol.* **222** (Pt, suppl. 1), jeb188854(2019).
49. S. Mansourian *et al*., Wild African Drosophila melanogaster are seasonal specialists on marula fruit. *Curr. Biol.* **28**, 3960–3968.e3 (2018).
50. A. J. Zera, R. F. Denno, Physiology and ecology of dispersal polymorphism in insects. *Annu. Rev. Entomol.* **42**, 207–230 (1997).
51. S. Goossens, N. Wybouw, T. Van Leeuwen, D. Bonte, The physiology of movement. *Mov. Ecol.* **8**, 5 (2020).
52. S. Tung *et al*., Simultaneous evolution of multiple dispersal components and kernel. *Oikos* **127**, 34–44 (2018).
53. P. M. Itskov, C. Ribeiro, The dilemmas of the gourmet fly: The molecular and neuronal mechanisms of feeding and nutrient decision making in Drosophila. *Front. Neurosci.* **7**, 12 (2013).
54. K. J. Leitch, W. B. Dickson, M. H. Dickinson, Drosophila wind-assisted dispersal. GitHub. https://github.com/kateleitch/drosophila_wind_assisted_dispersal. Deposited 11 April 2021.